Non-Linear Internal Waves Pulse Cold Water Into the Shallow Inner-Shelf and Surfzone

Gregory Sinnett, Presenting Author and Falk Feddersen, Drew Lucas, Geno Pawlak and Eric Terrill

Scripps Institution of Oceanography,
University of California San Diego
gsinnett@ucsd.edu

Abstract

Non-linear internal waves (NLIW) are known to transport cold, nutrient rich water into the shallow inner-shelf. However, the evolution of NLIWs into the very shallow nearshore environment (< 15 m) has not been well resolved. Here, we present new observations of NLIW in water < 15 m using a dense array of thermistors and ADCPs to track NLIW propagation all the way to the shore. Multi-day periods of enhanced internal wave activity were observed, with oscillations at semi-diurnal (12 h) and first harmonic (6 h) periods surging cold water inshore at a variety of different angles. Temperature variations as large as 2°C in 30 min, and at periods sometimes < 9 min were associated with internal wave events in water as shallow as 7 m. Occasionally, NLIWs were observed to propagate all the way to the surfzone, temporarily decreasing the water temperature by as much as 3 degrees in 1 m water depth, and leaving a residual cooling signature that persisted long after the end of the internal wave event.

1 Introduction

Internal waves (internal isopycnal oscillations) are ubiquitous on coasts worldwide, including in the Southern California Bight. Nearshore (depth < 15 m) nonlinear internal waves (NLIW) (e.g., Winant, 1974; Pineda, 1991; Omand et al., 2011; Walter et al., 2014b), often identified as onshore propagating surface slicks (convergence zones), can drive nearshore temperature fluctuations of up to 6°C at tidal and higher frequencies. Internal waves on continental shelves have many possible generation mechanisms, including large-scale tidal flow or inertial frequency forcing Shroyer et al. (2011), and may be either locally or remotely generated Nash et al. (2012). Nearshore nonlinear internal waves can have significant temporal variation (e.g., Suanda and Barth, 2015) that depends on many factors such as the background stratification across the shelf (e.g., Zhang et al., 2015), subtidal circulation, and barotropic tides. NLIW have significant associated turbulence, often elevated on the NLIW trailing edge Walter et al. (2014a). NLIW have been tracked via remote-sensing to ≈ 7 m depth Suanda et al. (2014). However, cross-shore internal wave transformation in shallow depths, all the way to the shoreline, and the associated transport and mixing that impact nearshore ecosystem have, until recently, not been resolved.

Internal waves impact nearshore ecosystem health through the material (e.g., heat, nutrients, larvae) transport and mixing. The general transport effectiveness of a NLIW depends upon many factors which change as the wave transforms across the nearshore. Thus, to understand the impact of NLIW on the nearshore, it is critical to understand the NLIW transformation (shoaling and dissipation) across the nearshore. Laboratory experiments of NLIW (bore) propagation in a two layer fluid on a slope reveal that

dense fluid is transported up the slope while density excess, layer thickness and speed all proportional to total water depth Wallace and Wilkinson (1988). These bores both dissipate (reduce their amplitude) and increase the fluid column potential energy through irreversible mixing. Two-layer NLIW-event model simulations reveal the structure of NLIW-associated turbulent dissipation and density mixing. The mixing efficiency (ratio of buoyancy flux and dissipation) depends on the internal Iribarren number (ratio of slope to wave steepness) Arthur and Fringer (2014). Similarly, the cross-shore transport induced by a 2-layer NLIW event also depends on internal Iribarren number Arthur and Fringer (2016). However, unlike these 2-layer laboratory and modeling studies, the nearshore ocean is continuously stratified, and the cross-shore NLIW transformation with continuous stratification has not been observed and is not understood. Here, we report on observations of nearshore NLIW events in an effort to understand their shoaling and transformation in water depth < 15 m.

2 Scripps Internal Waves Experiment

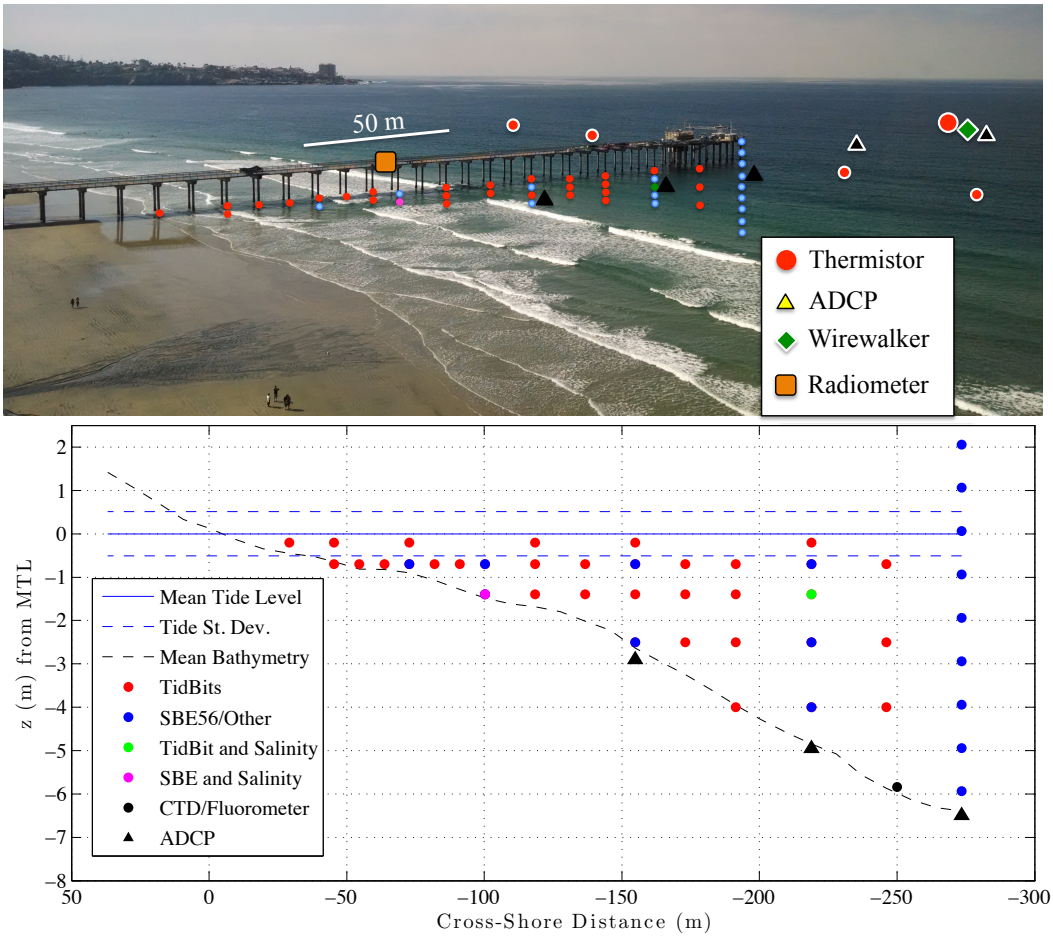

Figure 1: **Top:** Photograph of the Scripps Institution of Oceanography (SIO) pier and adjacent nearshore waters. Approximate sensor locations are indicated. **Bottom:** Detail of the instruments deployed in 7 m depth and shallower. The cross section is looking south, with an average bathymetric profile (black dotted line) and mean tide level and standard deviation (blue solid and dotted lines respectively.)

Internal waves were observed at Scripps Beach (in the Southern California Bight) from

15 m depth to the shoreline with a suite of temperature and velocity measurements taken between 29 Sept - 29 Oct. During this time, 36 Hobo TidBit and 8 Seabird SBE56 thermistors were deployed on the Scripps Institution of Oceanography (SIO) pier pilings at various cross-shore and vertical locations (see Fig 1). These TidBits and SBE56s sampled at 3 min and 15 s, respectively. All thermistors were calibrated in the SIO Hydraulics Laboratory temperature bath, yielding accuracies of 0.01°C and 0.003°C for the TidBits and SBE56s respectively. A pier-end (≈7 m depth) vertical thermistor chain with 1 m vertical resolution maintained by the SIO Coastal Observing Research and Development Center (CORDC) provided additional high-resolution and highly-accurate temperature measurements at 1 Hz sampling rate. Water column velocity was observed by three upward looking Nortek Aquadopp current profilers deployed in depths from 3 - 7 m at cross-shore locations (relative to a mean tidal extent) $x = -155$ m, $x = -219$ m, and $x = -275$ m with 1 min averaged sampling and vertical bin sizes of 0.3 m, 0.3 m and 0.5 m, respectively. Additional meteorological, tide, and wave measurements were made at the end of the pier.

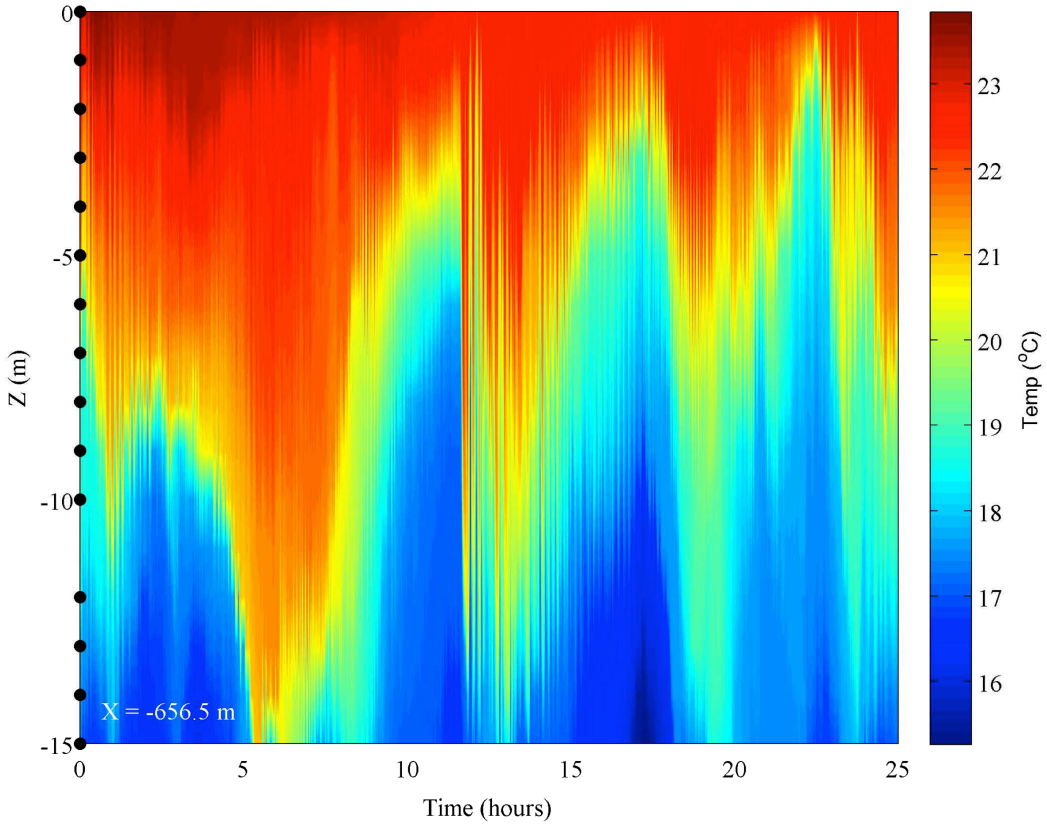

Figure 2: Temperature as a function of time and vertical Z at the 15-m depth mooring over 25 hours starting 6 Oct 2014. Black dots represent thermistor vertical locations.

Additional instrumentation deployed between 15 m water depth and the pier end was designed to study internal wave cross-shore transformation across the entire nearshore ($<$ 15 m depth). Four SBE56 thermistors were mounted on the bottom ($\approx$ 7 m water depth, $x = -275$ m) at alongshore locations spaced 100 m apart and sampling at 1 Hz to capture incident internal wave angle relative to the slope. An upward-looking 5-beam ADCP (Teledyne Sentinel V) capable of resolving vertical motions, and moored

temperature chain consisting of SBE56 thermistors spaced vertically every meter sampling at 2 Hz were deployed in 15 m depth ($x = -675$ m).

3 Nonlinear Internal Wave Examples

Internal wave events were observed in 15-m depth as pulses of near-bottom cold water at semi-diurnal and higher frequencies. On 6 Oct 2014, a train of four large NLIW events arrived at the 15 m isobath over 24 h (Fig. 2) and propagated onshore - some all the way to the surfzone - with a highly baroclinic velocity structure. On this day, surface gravity waves were small (significant wave height of 0.5 m) with a moderately high spring tide. These NLIW events were notably not at a semi-diurnal tidal period, but rather the first harmonic, near 6 hours. Each large NLIW event is characterized by a period of cooling beginning near the bottom and extending up to $z \approx -2$ m lasting approximately 4 hours. An abrupt period of warming follows each event, and returns the bottom to a temperature that is colder after the passage of each subsequent wave, indicating some irreversible mixing. Qualitatively, these NLIW events are similar to those observed in 15 m depth in Monterey Bay Walter et al. (2012).

During these large NLIW events, high frequency temperature variability is also observed, particularly between hours 14–18 (Fig. 3) associated with one of the large NLIW events (Fig. 2). This high-frequency temperature variability can have oscillations of 1.5 °C, at periods of ≈ 10 min, and is coherent over nearly the entire water column.

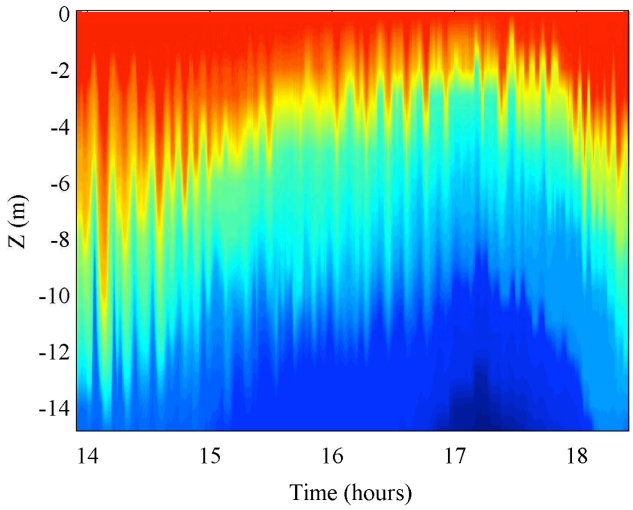

Figure 3: Temperature as a function of time and vertical Z at the 15-m depth mooring over 5 hours corresponding to time 14–19 hr from Fig. 2 with same temperature scale. The high frequency temperature oscillations have a period of approximately 9 minutes.

A subset of these large NLIW events can be tracked from 15 m depth all the way to the surfzone (Fig. 4). As the four large NLIW events in 15-m depth propagated onshore and transformed, their temperature signature was observed at pier-end ($x = -274$ m, Fig. 4e). The first (and weakest) NLIW event (hours 2–3) did not continue to propagate onshore, however NLIW events 2–4 propagated onshore coherently past the surfzone boundary ($x = -118$ m, Fig. 4b), and into the surfzone in 0.7 m water depth (Fig. 4a). Coherent onshore propagation of two NLIW features is highlighted near hours 17 and 21 in Fig. 4

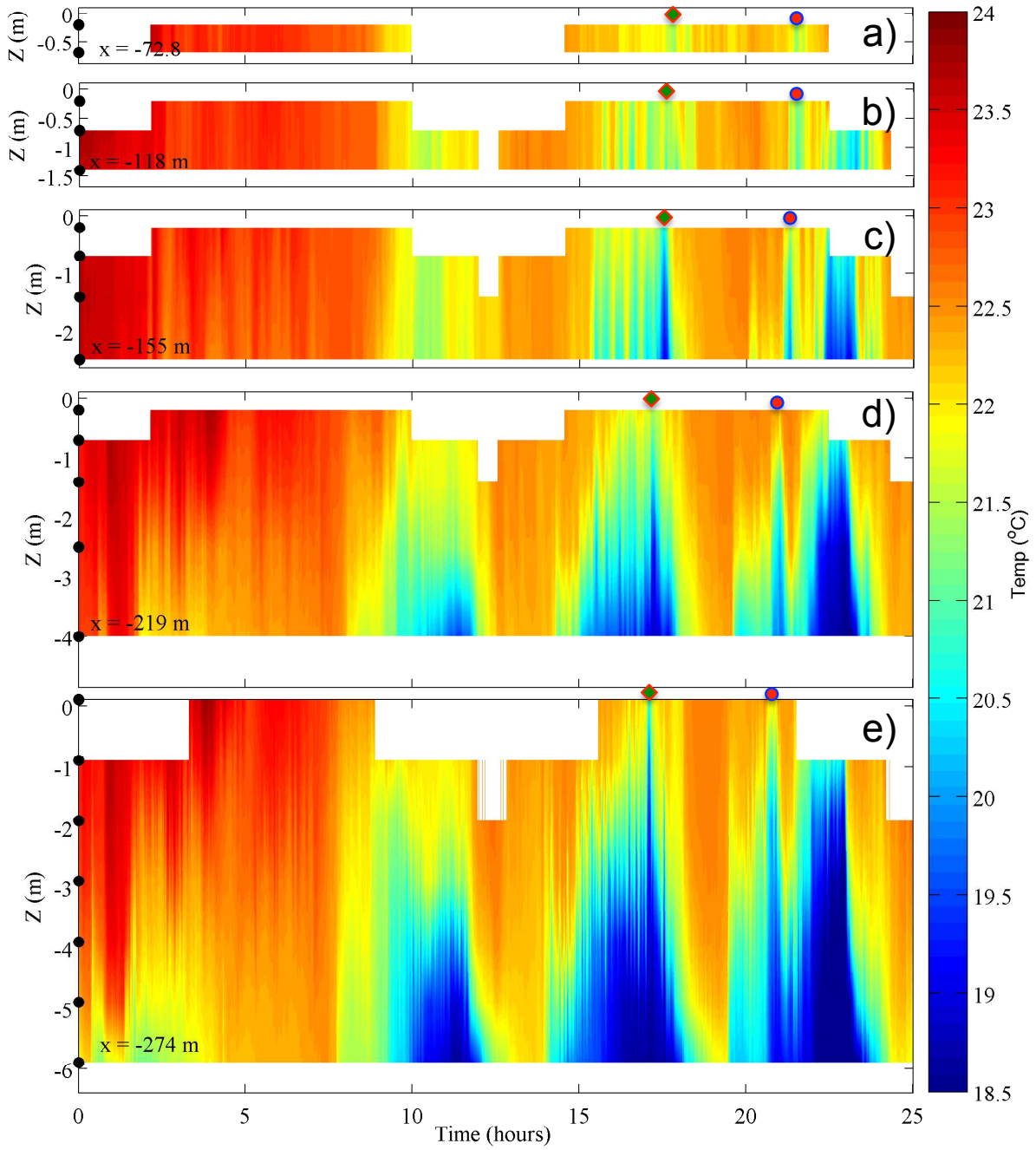

Figure 4: Temperature as a function of time and vertical Z on 6 Oct 2014 (corresponding to Fig. 2) at various cross-shore locations from (top) most-onshore to (bottom) most offshore. The cross-shore locations are indicated in each panel. The vertical axis is scaled equally between all plots to accurately represent the local depth at each cross-shore location, and the black dots represent the vertical thermistor locations. Two NLIW features are highlighted (orange diamond and magenta circle) to indicate onshore propagation. Note this colorscale is different than in Fig. 2.

(diamonds and circles), allowing NLIW propagation speed estimation. Over the course of these NLIW events, the mid-water temperature fluctuation, ΔT, in 4-m depth was 3°C . Farther onshore ΔT is weaker, indicating a loss of NLIW amplitude (e.g., Fig. 4). Similar to 15-m depth (Fig. 2), in depth $\geq$2.5 m, NLIW retreat was more rapid than arrival and

cold waters rapidly warmed (e.g., hours 18–19, Fig. 4d,e). However within the surfzone after NLIW retreat (hours 18–19, Fig. 4a,b), colder water persisted indicating that colder NLIW water was irreversiblely mixed and left behind.

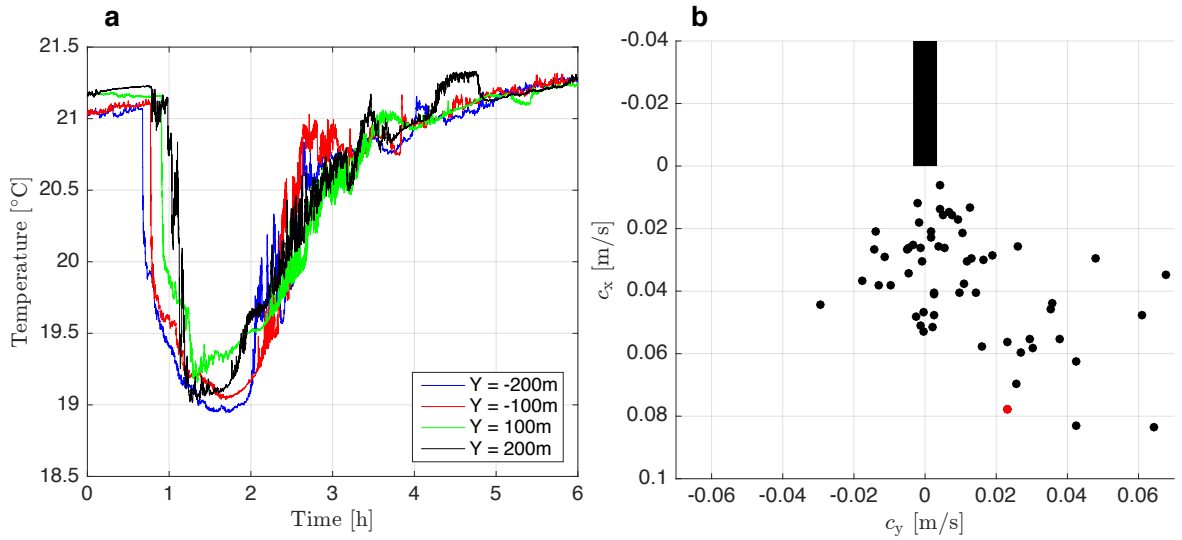

Figure 5: (a) Near-bottom temperature in ≈ 7m depth versus time (relative to 26 Oct 2014 8:45pm PDT) at four alongshore locations as indicated in the legend. Note the progressive onset of the roughly 2 °C temperature decrease just before hour 1. During the recovery, high frequency temperature variability is observed at all location between hours 2 and 3. The event is nearly adiabatic at this location. (b) Across-shore (x) and Along-shore (y) internal wave velocity observed near the pier end for all waves present in the one-month sampling period. The wave event detailed on the left is shown in red. For visualization purposes, the pier is indicated at the origin (thick black line) to highlight the choice of coordinate system (+x onshore and +y to the north).

Another example of NLIW propagation (from 26 Oct) demonstrates that these NLIWs can be obliquely incident in water as shallow as 7 m. Near bottom temperature from four alongshore locations dropped rapidly and then recovered over a six hour period, typical of a NLIW event (Fig. 5a). However, each temperature sensor recorded the sharp onset (> 0.16 °C/min) at different times. The internal wave front arrived at Y = -200 m at t = 40 min, passed by each subsequent sensor, and eventually arrived at Y = 200 m roughly 21 minutes later. The internal wave front was also propagating in the x direction at the same time (not shown) allowing for an estimate of phase speed and angle. The recovery in temperature does not follow the same pattern as the onset of the event. Whereas the initial temperature drop took only several minutes, the recovery takes 1-2 hours and begins at different times, indicating a receding wavefront that is not as uniform. The recovery contains a "turbulent period" (between hour 2 and 3) where temperatures rapidly oscillate 0.5 °C over 90 s. Similar NLIW retreat characteristics have been observed at the 15 m isobath in Monterey Bay Walter et al. (2012, 2014a) and in modeling studies Arthur and Fringer (2014).

The X and Y components of phase speed (c_x and c_y) for all waves observed in this experiment are shown in Fig. 5b, with the example in (a) shown in red. The coordinate system chosen here makes the top of the plot the coast (east) and the pier is indicated by the black rectangle. The majority of the faster moving NLIW events originate from the

south-west. This is in the direction of the southern terminus of La Jolla Canyon, and may be a likely generation spot for internal waves observed in this region's nearshore waters.

4 Summary

Non-linear internal waves were observed for a 1 month period in the fall of 2014 at Scripps Beach in Southern California. Internal wave events observed at the 15 m isobath contained energy at the semi-diurnal band, and also occasionally at the 6 hour first harmonic. This internal wave energy was observed to propagate onshore, with occasional cold signals observed in water less than 1 m deep. NLIW events were observed to propagate onshore with a variety of phase speeds and from a variety of angles. However, the majority of events with phase speeds above 0.05 $\mathrm{m\,s^{-1}}$ were traveling toward the north-east.

References

Arthur, R. S. and Fringer, O. B. (2014). The dynamics of breaking internal solitary waves on slopes. *J. Fluid Mech.*, 761:360–398.

Arthur, R. S. and Fringer, O. B. (2016). Transport by breaking internal solitary waves on slopes. *J. Fluid Mech.*, 789:93–126. doi:10.1017/jfm.2015.723.

Nash, J. D., Kelly, S. M., Shroyer, E. L., Moum, J. N., and Duda, T. F. (2012). The unpredictable nature of internal tides on continental shelves. *J. Phys. Ocean.*, 42(11):1981–2000.

Omand, M. M., Leichter, J. J., Franks, P. J. S., Lucas, A. J., Guza, R. T., and Feddersen, F. (2011). Physical and biological processes underlying the sudden appearance of a red-tide surface patch in the nearshore. *Limnol. Oceanogr.*, 56:787–801.

Pineda, J. (1991). Predictable upwelling and the shoreward transport of planktonic larvae by internal tidal bores. *Science*, 253(5019):548–551.

Shroyer, E., Moum, J., and Nash, J. (2011). Nonlinear internal waves over New Jersey's continental shelf. *J. Geophys. Res.*, 116(C03022).

Suanda, S. H. and Barth, J. A. (2015). Semidiurnal baroclinic tides on the central Oregon inner shelf. *J. Phys. Ocean.* doi: 10.1175/JPO-D-14-0198.1.

Suanda, S. H., Barth, J. A., Holman, R. A., and Stanley, J. (2014). Shore-based video observations of nonlinear internal waves across the inner shelf. *Journal of Atmospheric and Oceanic Technology*, 31:714–728.

Wallace, B. and Wilkinson, D. (1988). Run-up of internal waves on a gentle slope in a two-layered system. *J. Fluid Mech.*, 191:419–442.

Walter, R. K., Squibb, M. E., Woodson, C. B., Koseff, J. R., and Monismith, S. G. (2014a). Stratified turbulence in the nearshore coastal ocean: Dynamics and evolution in the presence of internal bores. *Journal of Geophysical Research: Oceans*, 119:8709–8730.

Walter, R. K., Woodson, C. B., Arthur, R. S., Fringer, O. B., and Monismith, S. G. (2012). Nearshore internal bores and turbulent mixing in southern Monterey Bay. *J. Geophys. Res.*, 117.

Walter, R. K., Woodson, C. B., Leary, P. R., and Monismith, S. G. (2014b). Connecting wind-driven upwelling and offshore stratification to nearshore internal bores and oxygen variability. *J. Geophys. Res., Oceans*, 119:3517–3534.

Winant, C. (1974). Internal surges in coastal waters. *J. Geophys. Res.*, 79(30):4523–4526.

Zhang, S., Alford, M. H., and Mickett, J. B. (2015). Characteristics, generation and mass transport of nonlinear internal waves on the washington continental shelf. *Journal of Geophysical Research: Oceans*, 120:741–758.